Earthquakes and Structures, *Vol. 17, No. 1 (2019) 91-99*
DOI: https://doi.org/10.12989/eas.2019.17.1.091

Probabilistic seismic risk assessment of simply supported steel railway bridges

Mehmet F. Yilmaz[*1], Barlas O. Caglayan[2a] and Kadir Ozakgul[2b]

[1]*Department of Civil Engineering, Ondokuz Mayıs University, Kurupelit 55139, Samsun, Turkey*
[2]*Department of Civil Engineering, Istanbul Technical University, Maslak 34469, Istanbul, Turkey*

(Received June 11, 2018, Revised April 15, 2019, Accepted May 17, 2019)

Abstract. Fragility analysis is an effective tool that is frequently used for seismic risk assessment of bridges. There are three different approaches to derive a fragility curve: experimental, empirical and analytical. Both experimental and empirical methods to derive fragility curve are based on past earthquake reports and expert opinions which are not suitable for all bridges. Therefore, analytical fragility analysis becomes important. Nonlinear time history analysis is commonly used which is the most reliable method for determining probabilistic demand models. In this study, to determine the probabilistic demand models of bridges, time history analyses were performed considering both material and geometrical nonlinearities. Serviceability limit states for three different service velocities were considered as a performance goal. Also, support displacements, component yielding and collapse limits were taken into account. Both serviceability and component fragility were derived by using maximum likely hood methods. Finally, the seismic performance and critical members of the bridge were probabilistically determined and clearly presented.

Keywords: railway bridge; fragility curve; nonlinear time history analysis; probabilistic seismic assessment

1. Introduction

In Turkey, there are three active earthquake zones named North Anatolia, Southeast Anatolia, and Western Anatolia. Approximately, 42% of its territory lies on the high seismic risk zones. Therefore, the seismic events seriously threat all structures and transportation lines in the big and industrialized cities of Turkey. On the other hand, in Turkey, there are many historical bridges, most of them registered as a national heritage. Transportation systems should continue to give service after a tremendous event such as an earthquake.

Railway lines have an important contribution to the economy with passenger, freight, mine and military transportation. The total length of the railway lines is approximately 12,000 km. The construction of railway lines dates back to the end of the 19th century that mean most of the parts of railway system are older than 100 years. So, possible damage or failure of the bridges may disrupt the service of railway lines. Thus, seismic performances of bridges need to be determined to sustain the continuity of railway transportation after seismic events.

There are many linear and nonlinear approaches to determine the seismic performance of bridges and fragility curve is one of the famous and effective tools for this aim (Pan *et al*. 2007). Fragility is the probability of exceedance of certain performance limit under seismic events of structural or nonstructural components. There are three methods to derive fragility curve; expert based, empirical and analytical. Past earthquake reports and expert opinions are used to derive expert-based and empirical fragility curves (Yazgan 2015). Required information to derive expert base and empirical fragility curve is not possible for many bridges. So, analytical fragility curves become important. The analytical method is dependent on some numerical analysis results such as elastic spectral analyses, nonlinear static analyses and nonlinear time-history analyses (Liu *et al*. 2017, Razzaghi *et al*. 2018, Sfahani and Guan 2018). These numerical analyses are used to construct a probabilistic seismic demand model (PSDM). Nonlinear time history analyses (NTHA) are the most reliable and time-consuming analysis methods to derive PSDMs (Banerjee and Shinozuka 2007, Bignell *et al*. 2004, Shinozuka *et al*. 2000a, b, Mackie and Stojadinovic 2001, Kumar and Gardoni 2014, Mosleh *et al*. 2016). Selection of earthquake data for NTHA is an important step to derive fragility curves because the local site condition of selected earthquake data has an important effect on NTHA's results (Sisi *et al*. 2018).

Performance criteria for bridges need to be determined to derive fragility curves. There are different approaches to specify performance criteria for bridges. Tsionis and Fardis (2014), Yilmaz and Caglayan (2018) used maximum horizontal rotation and displacement limit given in Annex A2 EN 1990 as service criteria which is important for railroad geometry and prevent derailment of the train. Mander (1999) conducted experimental studies on bridge

*Corresponding author, Ph.D.
E-mail: yilmazmehmet3@itu.edu.tr
[a]Associate Professor
E-mail: caglayan@itu.edu.tr
[b]Associate Professor
E-mail: ozakgulk@itu.edu.tr

ISSN: 2092-7614 (Print), 2092-7622 (Online)

supports and determined the displacement values corresponding to the performance targets. Mohseni (2012) considered bending curvature ductility for steel superstructure elements.

In this study, a simply supported steel truss railway bridge was considered. Thirty different real earthquake data were selected by considering three different soil conditions. The selected data were scaled from 0.1 g to 1.0 g, and totally 300 different nonlinear times history analyses were performed to determine seismic response of this bridge. As for performance limit, support displacements, component yielding and collapse, and service limits were defined. The service condition was determined for three different service velocities. For supports, four different performance criteria were determined as slight, moderate, large and collapse. Also, two different performance criteria were defined for truss components; yielding and collapse. Median values and dispersions of all conditions were carried out, and the obtained results were compared with previous existing studies in the literature.

2. Analytical method and simulation

Probability of exceeding performance limits for structure or structural components are determined in terms of intensity measure (*IM*). Fragility can be express as Eq. (1) (Padgett and DesRoches 2008).

$$Fragility = P[EDP \geq C \mid IM] \tag{1}$$

where P is the probability of the particular case, EDP is the engineering demand parameter and C is the capacity. Probabilistic seismic demand models (*PSDMs*), structural demand and capacity are determined by using nonlinear time history analysis to model and analyze the bridge structure.

2.1 Probabilistic seismic demand model

A PSDM describes the seismic demand of a structure or structural component in terms of an approximate IM (Padgett and DesRoches 2008)

$$P[EDP \geq d \mid IM] = 1 - \phi\left(\frac{\ln(d) - \ln(\widehat{EDP})}{\beta_{EDP|IM}}\right) \tag{2}$$

where the median EDP is estimated as a power model

$$\widehat{EDP} = aIM^b \tag{3}$$

or a linear logarithm model

$$\ln(EDP) = \ln(a) + b\ln(IM) \tag{4}$$

where a and b are regression coefficients, ϕ is the standard normal cumulative distribution function, $\widehat{EDP}$ is the median value of engineering demand, d is the limit state to determine the damage level, and $\beta_{EDP|IM}$ (dispersion) seen below is the conditional standard deviation of the regression (Siqueira *et al*. 2014)

$$\beta_{EDP|IM} \cong \sqrt{\frac{\sum(\ln(d_i) - \ln(aIM^b))^2}{N-2}} \tag{5}$$

2.2 Component and system fragility

Component fragility describes the seismic behavior of different components under the same level of damage and allows the weakest bridge component to be determined. In this study, all the elements of the main bridge truss and its supports were considered. Capacities of elements of truss system were calculated under tension, compression, and bending.

However, the point of system fragility is to determine all possible damage probabilities which can occur on the structural system, since all components must be considered to derive the overall bridge fragility curve. Bridge damage probability for a chosen limit state is the union of probabilities of each component for the same limit state (Nielson and DesRoches 2007). Upper and lower first-order bounds on the system give a proper opinion for the fragility curve representing the whole bridge system. For a structural serial system, upper and lower bound fragility curves can be obtained by deriving all the component fragilities and collecting them into the Eq. (6). Maximum of component failure probability provides the lower bound and assumes that there is a certain correlation between the component demands and gives unconfident results. Despite the upper bound assumes no correlation between the component demands, it gives conservative results (Nielson and DesRoches 2007).

$$\max_{i=1}^{n}[P(F_i)] \leq P(F_{system}) \leq 1 - \prod_{i=1}^{m}[1 - P(F_i)] \tag{6}$$

where $P(F_i)$ is the failure probability of component i, and $P(F_{system})$ is the failure probability of the system.

3. Bridge description

The bridge considered in this study is a simply supported steel truss bridge having 40 m length of span and is composed of main trusses, floor beams, stringers, upper and bottom lateral bracings on the Malatya-Cetinkaya railway line, located about 70 km east of Malatya city and was built by the Maschinenfabrik Augsburg Nürnberg A.G. Werk Gustavsburg company in 1935. Horizontal curve radius of the road is 300 m and applied by the rail placement on the bridge, and to overcome the

Fig. 1 General view of the bridge

Table 1 Properties of selected earthquake data

A Ground Side Earthquake Data						B Ground Side Earthquake Data						C Ground Side Earthquake Data					
Earthquake	Data	Moment Magnitute (Mw)	Record	PGA (g)	Center Distance (km)	Earthquake	Data	Moment Magnitute (Mw)	Record	PGA (g)	Center Distance (km)	Earthquake	Data	Moment Magnitute (Mw)	Record	PGA (g)	Center Distance (km)
Morgan Hill	24.02.1984	6.2	G01320	0.098	16.2	Coyote Lake	06.08.1979	5.8	G06230	0.4339	3.1	Coyote Lake	06.08.1979	5.7	G02140	0.339	7.5
Coyote Lake	06.08.1979	5.7	G01320	0.132	9.3	Northridge	17.01.1994	6.7	ORR090	0.5683	22.6	Coyote Lake	06.08.1979	5.7	G03050	0.272	6
Landers	28.06.1992	7.3	ABY090	0.146	69.2	Loma Prieta	18.10.1989	7.1	CLS000	0.6437	5.1	Coyote Lake	06.08.1979	5.7	G04270	0.248	4.5
Loma Prieta	18.10.1989	6.9	G01090	0.473	11.2	Livemor	27.01.1980	7.4	LMO355	0.252	8	Imperial Valley	15.1.1979	7	J-ELC180	0.313	8.3
N. Palm Springs	08.07.1986	6	AZF225	0.099	20.6	N. Palm Springs	08.07.1986	6	DSP000	0.331	8.2	Imperial Valley	15.10.1979	7	H-AEP045	0.327	8.5
N. Palm Springs	08.07.1986	6	ARM360	0.129	46.7	Northridge	17.01.1994	6.7	TPF000	0.364	37.9	Imperial Valley	15.10.1979	7	H-BCR230	0.775	2.5
N. Palm Springs	08.07.1986	6	H02090	0.093	45.6	San Fernando	02.09.1971	6.6	ORR021	0.324	24.9	Imperial Valley	15.10.1979	6.5	H-CX0225	0.275	10.6
Whittler Narrows	01.10.1987	5.3	MTW000	0.123	20.4	Whittler Narrows	10.01.1987	6	ALH180	0.333	13.2	Cape Mendocino	25.04.1992	7.1	PET090	0.662	9.5
Anza (Horse Cany)	25.02.1980	4.9	PTP135	0.131	13	Kocaeli	17.08.1999	7.4	SKR090	0.376	3.1	Loma Prieta	18.10.1989	6.9	HCH090	0.247	28.2
Anza (Horse Cany)	25.02.1980	4.9	TVY135	0.081	5.8	Victoria, Mexica	09.06.1980	6.1	CPE045	0.62	34.8	Loma Prieta	18.10.1989	6.9	G02000	0.367	12.7

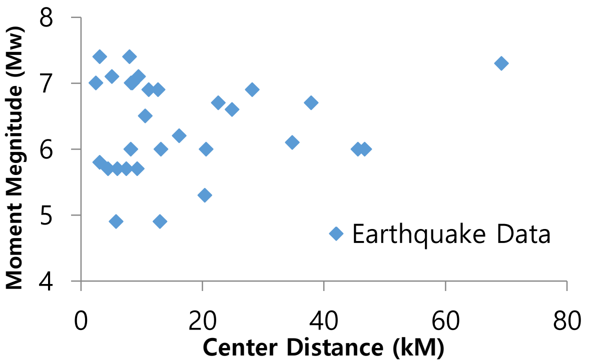

Fig. 2 Distribution moment magnitude to their center distance of selected earthquake data

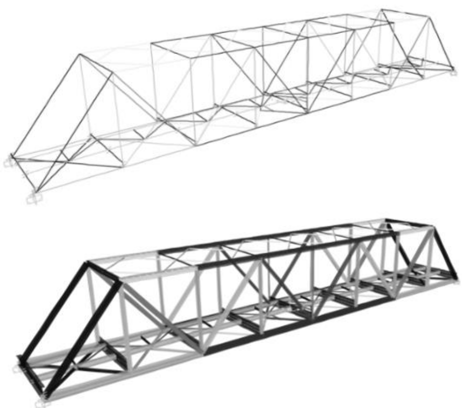
Fig. 3 3D FE model views of the bridge

centrifugal forces inner and outer trusses were designed for related different strength. The structural bridge members are designed by using only angles as well as constructing built-up sections. There are walkways on both sides of the sub-spans, and the sleepers rest over stringers mounted to the transverse girders. A general view of the bridge is given in Fig. 1.

4. Analytical modeling and simulation.

4.1 Ground motion suites

The effect of ground motion on any structure can be obtained using a linear or nonlinear mathematical model. Nonlinear time history analysis is used to minimize structural response uncertainties and provides an accurate relationship between ground motion IMs and EDPs. So, in this study, incremental dynamic analysis (IDA) method was used (Vamvatsikos and Allin Cornell 2002). All responses of the bridge were obtained to derive fragility curves and to determine its seismic performance.

30 different real earthquake data were selected considering different soil types naming A, B, and C, as well as their moment magnitudes, PGAs and epicentral distances "distance between seismogram and earthquake center". The moment magnitudes, PGAs and central distances of records are varying between 4.9-7.4, 0.08-0.78 g and 2.5-69.2 km, respectively. The distribution of moment magnitudes to center distances is shown in Fig. 2. The selected earthquake data were scaled to 10 different PGA from 0.1 g to 1.0 g, and 300 different nonlinear time history analyses were totally performed for the truss bridge considered in this study. Properties of selected earthquake data are shown in Table 1.

4.2 Analytical bridge model

FE model of the truss bridge was generated by using 2-node 3D beam elements, springs and link elements for structural members, supports and connections based on the existing shop drawings of the related bridge and in-situ visual inspections. Due to the differences between the centerlines of transverse and stringer, rigid bar elements were used to model the eccentricity between these two components in the FE model. While the weight of the sleepers and rails was considered as dead load and mass at the appropriate nodes, the weight of perforated plates and

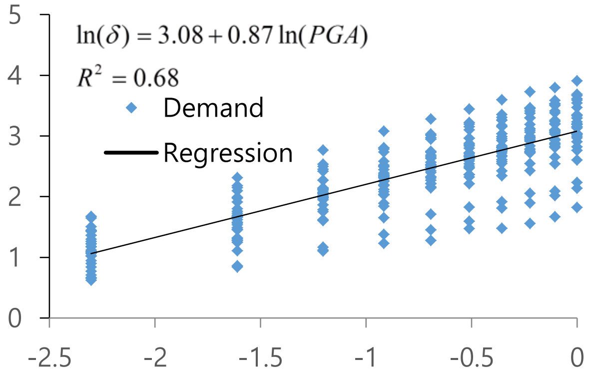

(a)

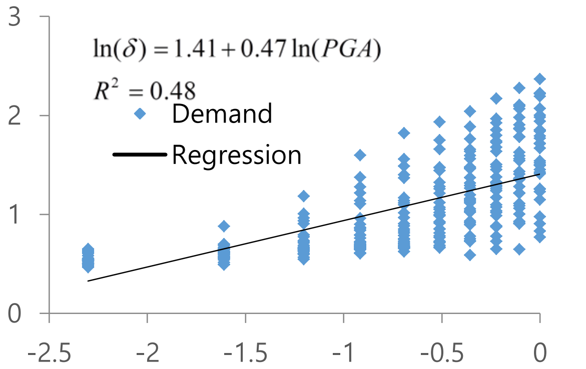

(b)

Fig. 4 PSDMs for pinned bearing (a) longitudinal direction, (b) transverse direction

gusset plates were included by increasing the weight of the bridge members 5%. Steel quality of the bridge members was defined as ST37 (S235) which is appropriate for the construction year of the bridge. Similarly, in another study presented by Larsson and Lagerqvist (2009), yield and ultimate strength for old railway and roadway steel bridges were taken as 200 MPa and 360 MPa, respectively. FE model created by using SAP2000 software was composed of 132 nodes, 202 frames, and 42 link elements. 3D FE model views of the bridge are shown in Fig. 3.

Time history analyses were applied to the model considering both material and geometric nonlinearities. The material nonlinearities were defined as steel fiber PMM plastic hinges at both end nodes and at the mid-points of all beam members of the bridge. Geometric nonlinearity was defined as P-Δ effects coupled with large displacement. For the solution of the dynamic equation of motion under the earthquake loads with three directions, Newmark's direct integration method was used in the time history domain analysis.

5. Demand models and performance limits

5.1 Probabilistic seismic demand models

PSDMs were constructed based on the peak transverse displacement at the mid-point and bearing of the bridge. The nonlinear time history analyses were employed for the IM selected as PGA. It was found that there is a good correlation between PGA and longitudinal displacement of the pinned bearing of the bridge. PSDMs of pinned bearings in the direction of longitudinal and transverse are shown in Fig. 4 and constants of Eq. (4) that obtained using the result of regression analysis are illustrated. The R^2 shows the convenience of the regression line and increase with the increasing convenience of analysis.

Table 2 Maximum angular variation and minimum radius of curvature (EN1990-prANNEX A2 2001)

Speed Range (km/h)	Rotation (rad)	Curvature (1/m)
V≤120	0.0035	1700
120<V≤200	0.0020	6000
V>200	0.0016	14000

Table 3 Quantitative limit states for bridge components in (mm) (Nielson 2005)

Component	Damage state			
	Slight Damage	Moderate Damage	Extensive Damages	Collapse Case
Low-steel pinned bearing-longitudinal	6	20	40	255
Low-steel pinned bearing-transverse	6	20	40	255
Low-steel sliding bearing-longitudinal	50	100	150	255
Low-steel sliding bearing-transverse	6	20	40	255

5.2 Serviceability limits estimation

As the serviceability limit state, the lateral displacements of the bridge were considered. Therefore, lateral displacement limits given in EN1990-Annex A2 for railway bridges (EN1990-prANNEX A2 2001), including maximum angular variation and minimum radius of curvature to limit lateral displacement for different velocities were used (see Table 2). In this case, bridge lateral deformation at the middle of the span was considered.

5.3 Components performance limits estimations

As the main causes of damage in steel truss bridges, buckling of the upper and lower lateral bracing members and shear failure of the transverse members can be considered (Bruneau *et al.* 1996, Kawashima 2012). Shah *et al.* (2009) presented a reliability assessment based on tension and compression capacities of members as the limit state for steel truss bridges. In most cases, the buckling capacity of a steel member is smaller than its tension capacity, so the compression capacity with bending moments was considered as a performance limit case during the calculation of the element limit state.

Determining the limit state for a different component of the bridge is an important step to derive a fragility curve. Four different limit state levels as slight, moderate and large/extensive damages/displacements and (finally) collapse case were defined by HAZUS-MH (FEMA 2003). Also, the timeline needed for the repair of a bridge is the key parameter to determine the limit state.

Each limit state describes the different level of bridge functionality over time. The limit states need to be functionally equivalent. Prescriptive approach is an effective tool to determine the limit state for different structural components. Limit states of steel bearings for highway bridges were determined by Mander (1999) and some of them are given in Table 3.

According to these limit states (Mander *et al*. 1996), 6 mm longitudinal deformation of a low- type pinned bearing caused cracks in the concrete pier, and this was supposed as the noticeable level of damage. For 20 mm deformation, prying of the bearings and severe deformation in the anchor bolts were predicted. At 40 mm toppling or sliding of the bearings was detected. It was believed that the bearing movement might exceed the 255 mm width causing a falling down from the seat and failure of the anchor bolt. In this case, the geometric continuity of superstructure lost and the collapse of the bridge system occurred.

6. Deriving fragility curve

Fragility function is mostly defined by two parameters log-normal distribution function. There are two different statistical approaches to determine this parameter, so-called method of finding the moment parameter and maximum likelihood method (Baker 2015). In this study, the nonlinear time history analysis was performed to determine the nonlinear behaviour of the bridge, and the maximum likelihood method was used to determine the fragility parameters. Fragility curve can be derived using Eq. (7).

$$P(C|IM = x) = \Phi\left(\frac{\ln(x/\theta)}{\beta}\right) \tag{7}$$

$P(C|IM=x)$ is the probability where a ground motion $IM=x$ will cause the structure to collapse. Φ is the standard normal cumulative distribution function (CDF), θ and β are median and standard deviation of the fragility function.

One of the most effective ways to calculate moments of EDP and IMs is the incremental dynamic analysis based on scaling each ground motion in a group until it causes structural failure. But this method has some difficulties. One of them is the need for the huge computational effort needed for the analysis. The other one is the unsuitable results obtained for the greater scale values that are used during the calculation which are not expected to occur for the site, and the last one, uncertainty representing that too large scaling small and medium ground motions do not produce a realistic result. One of the solutions is limiting of the ground motion scaling to a valuable IMs, and it is called a truncated incremental dynamic analysis (Baker, 2015). Maximum likelihood method was used to figure the likelihood of observed data so that a candidate fragility curve was derived.

$$Likelihood = \phi\left(\frac{\ln(IM_i/\theta)}{\beta}\right) \tag{8}$$

Table 4 Median and dispersion values for MSSS steel roadway bridge (PGA, g) Nielson (2005)

	Damage Levels			
	Slight	Moderate	Large	Collapse
Median	0.24	0.45	0.58	0.85
Dispersion	0.50	0.50	0.50	0.50

Table 5 Median and dispersion values for serviceability fragility curve based on train velocity (PGA, g)

		Damage Levels (km/h)		
		V<120	120<V<200	200<V
Serviceability Limit	Median	0.81	0.07	-
	Dispersion	0.36	0.73	-

$$\{\hat{\theta},\hat{\beta}\} = \arg\max_{\theta,\beta} \sum_{j=1}^{m}\left[in\phi\left(\frac{In(IM/\theta)}{\beta}\right)\right] + [n-m]In\left[1-\Phi\left(\frac{In(IM_{\max}/\theta)}{\beta}\right)\right] \tag{9}$$

Using Eq. (9) the fragility function parameters were obtained by maximizing the likelihood function.

Nielson (2005) determined median and standard deviation values of different roadway bridge considering four different damage levels. Table 4 shows the median and dispersion values for a multi-span simply supported (MSSS) steel roadway bridge.

6.1 Fragility curve for railway serviceability

Railway lines must have certain geometric characteristics in order to preserve traffic safety. Lack of these characteristics can cause serious events such as derailment as well as the overturning of a train. Three of such events were observed for the Kocaeli, Turkey earthquake (Byers 2004). In the specification, there is a geometric limitation for serviceability of railway line considering three different train speeds (EN1990-prANNEX A2 2001). Railway transportation is of great importance both nationally and internationally for passenger and goods transportation. Service speed affects transport capacity and quality (Lindfeldt 2015). Three different speed limits shown in Table 2 were used in this study and both median and dispersion values were calculated as well as fragility curves were derived. Table 5 shows the median and dispersion values and Fig. 5 shows serviceability fragility curves.

Fig. 5 shows the probabilities exceeding of serviceability limit states for PGA values. Nielson (2005) determined median values for multi-span simply supported (MSSS) steel girder roadway bridge as 0.24 g for slight damage, 0.45 g for moderate damage, 0.58 g for large damage and 0.85 g for collapse damage condition. Serviceability limit states were assumed as slight damage. (Tsionis and Fardis 2014).

Median values for slight damage of MSSS steel roadway bridges are 0.24 g which is higher than median values for serviceability limit of 120<V<200 km/h and

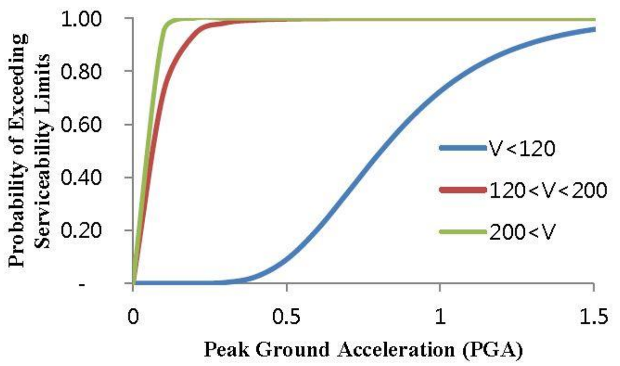

Fig. 5 Serviceability fragility curves

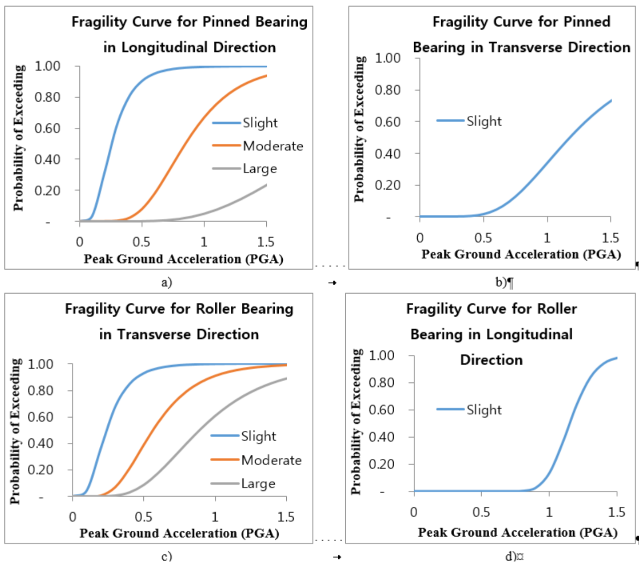

Fig. 6 Fragility curves for steel bridge bearings

V>200 km/h velocity limit, but smaller than serviceability limit for *V*<120 km/h. A PGA value of %10 probability of exceeding in 50 years is 0.41g according to Turkish seismic risk map. Probability of exceeding serviceability limit state for these values are %100, %99 and %2 for *V*>200 km/h, 200>*V*>120 km/h and *V*<120 km/h respectively. Probability of exceeding the same hazard level for MSSS steel roadway bridge are %85, %41 %23 and %7 for slight, moderate, extensive and collapse damage level respectively. Median values for the steel railway bridges, 200 >V>120 km/h service velocity and MSSS steel roadway bridge slight damage is close to each other but the steel railway bridge V<120 km/h service velocity higher than MSSS steel roadway bridge slight damage.

6.2 Fragility curves for bridge components

In this study median and dispersion values of the support displacements obtained from the nonlinear time history analyses were calculated by using maximum likelihood methods, as shown in Table 6.

Longitudinal and transverse displacement limits for four different damage levels are previously shown in Table 3. For pinned bearing longitudinal direction and roller bearing transverse direction, all displacements were smaller than

Table 6 Median and dispersion values for the steel railway bridge bearings (PGA, g)

		Damage Levels			
		Slight	Moderate	Large	Collapse
Pinned Bearing Longitudinal	Median	0.26	0.85	2.07	-
	Dispersion	0.51	0.37	0.44	-
Pinned Bearing Transverse	Median	1.18	-	-	-
	Dispersion	0.39	-	-	-
Roller Bearing Longitudinal	Median	1.15	-	-	-
	Dispersion	0.13	-	-	-
Roller Bearing Transverse	Median	0.24	0.56	0.89	-
	Dispersion	0.51	0.43	0.42	-

Table 7 Median and dispersion values for component fragility curve (PGA, g)

		Damage Levels	
		Yielding	Collapse
Transverse	Median	1.03	-
	Dispersion	0.27	-
Truss Bottom Beam	Median	1.23	-
	Dispersion	0.30	-
Truss Brace	Median	1.50	-
	Dispersion	0.42	-
Port Beam	Median	1.18	-
	Dispersion	0.42	-
Top Wind Brace	Median	0.43	0.71
	Dispersion	0.54	0.56

collapse limit state so median values and dispersion values cannot be calculated. For pinned bearing transverse direction and roller bearing longitudinal direction all displacements were smaller than moderate, large and collapse limit state so that median and dispersion values could not be calculated.

Median values for pinned bearing transverse direction and roller bearing longitudinal direction were calculated as 1.18 g and 1.15 g, respectively, and they were the highest values as well as safer than others. Median values for pinned bearing in longitudinal and roller bearing in transverse were 0.26 g and 0.24 g respectively. Fragility curve of pinned and roller steel bearings are shown in Fig. 6.

Element buckling capacities were calculated using AISC 360-10 (2016) specification, assuming axial forces coupled with bending acting on the bridge components. This consideration was used to specify whether damage occurred on the structural component or not. Median values and dispersion values are given in Table 7.

The smaller median values for yielding were obtained at top wind bracing as 0.43 g as well as 0.71 g for collapse. Median values for MSSS steel roadway bridge was 0.24 g and 0.85 g for slight damage and in case of collapse damage, respectively. Median values for yielding at the top wind bracing were higher than slight damage of MSSS steel bridge and similarly, median values for the collapse of top wind bracing were close to collapse damage of MSSS steel bridge. Fragility curves for damages resulted from yielding

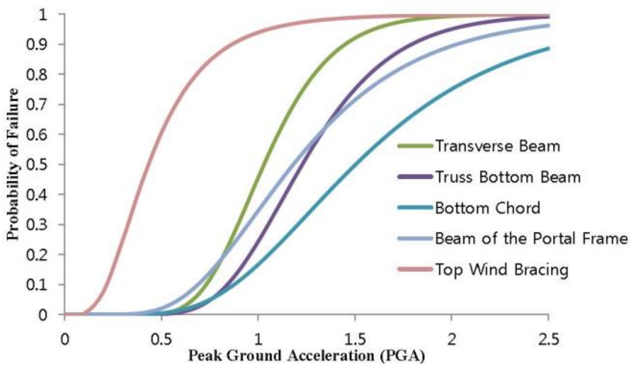

Fig. 7 Component fragility curves for yielding

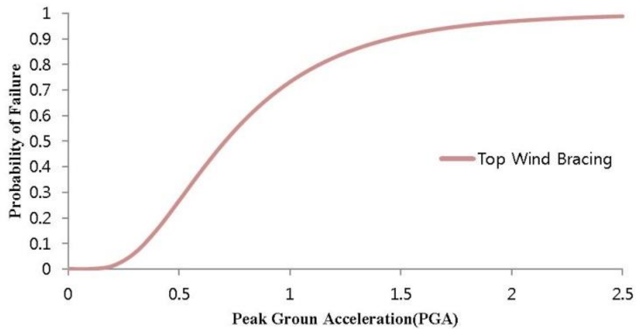

Fig. 8 Component fragility curve for the collapse

and the collapse of the bridge components are given in Figs. 7 and 8.

Top wind brace damage is more likely apparent than other component and there is no yielding observed at truss top beam, stringer, and bottom wind brace. And the only component that collapse damage observed is the top wind brace for the truss superstructure.

6.3 Fragility curve for the bridge system

Fragility curve of the entire bridge can be derived from a different approach. Upper and lower bound approaches were constituted as the two limits of the fragility curve. For a serial system, the bounds can be expressed as in Eq. (10).

$$\max_{i=1}^{n}[P(F_i)] \leq P(F_{system}) \leq 1 - \prod_{i=1}^{m}[1 - P(F_i)] \qquad (10)$$

Where $P(F_i)$ is the failure probability of component i, and $P(F_{system})$ is the failure probability of the system.

Maximum of component failure probability provides the lower bound (Nielson and DesRoches 2007). Since there is some correlation between component demands, this provides a non-conservative result. In contrast, the upper bound assumes no component correlation and hence provides a conservative result. The actual system fragility curve is expected to lie between the upper and lower bound curves. If only one component significantly affects system fragility, the bounds become closer, whereas if many components affect the system, the bounds can become wider (Nielson and DesRoches 2007). System fragility curves depends on support conditions are shown in Fig. 9 and system fragility curves depends on bridge members'

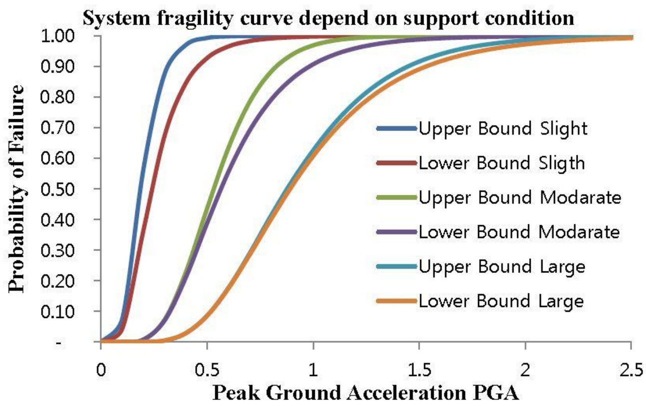

Fig. 9 System fragility curves depends on the support condition

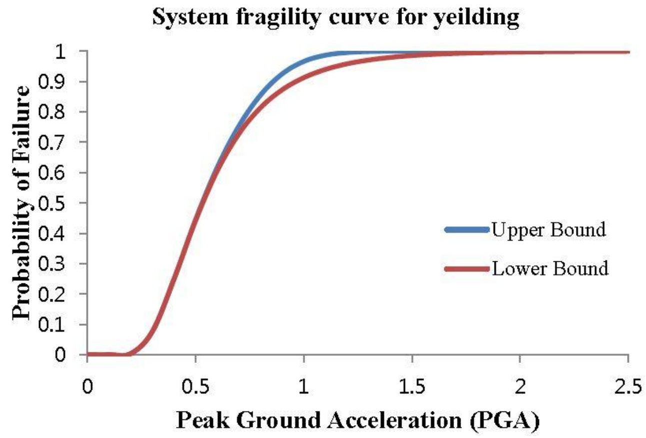

Fig. 10 System fragility curves for yielding of the component

yielding are shown in Fig. 10.

Probabilities of exceeding limit state for the PGA values of %10 probability of exceeding in 50 years are %97, %23, %3 and %0 for slight, moderate, large, and collapse damage based on upper bound, respectively. Comparing with MSSS steel roadway bridge, steel truss bridge is more vulnerable to slight damage but more conservative for moderate, large and collapse damage state.

Probability of exceeding limit state for the PGA values of %10 probability of exceeding in 50 years is %44 for yielding limit state of the truss component based on upper bound. This gives a similar result to MSSS steel roadway bridge moderate damage probability.

7. Conclusions

This study presents a probabilistic seismic assessment of a simply supported steel truss railway bridge. 3D finite element model of the bridge was generated by using SAP2000 software. 30 different real earthquake data were selected from A, B, and C ground sides. All the data were scaled to 10 different PGA intensity measures between 0.1 g to 1.0 g. A great number of the nonlinear time history analyses were performed to determine the nonlinear response of the bridge and its components. To derive fragility curves, various limit states such as serviceability, support damages, bridge members' yielding, and collapse were considered. Two parameters (median and dispersion) log-normal distribution functions were calculated by using the maximum likelihood method.

Serviceability fragility curves were derived for three different velocity limits. It was found that the increases in the service velocity increase the probability of failure. And V<120 km/h service velocity was calculated as much safer than the other two velocity limit state. Probabilities of failure for %10 probability of exceeding in 50-years earthquake intensity measures were calculated for 200<V, 200<V<120, and V<120, respectively. The results show that service velocity of the bridge needs to be limited to sustain traffic safety of railway line.

Four limit states for pinned and roller bearings were considered. Pinned bearing longitudinal and roller bearing transverse directions were obtained as most vulnerable to failure of the support and bridge system. Probabilities of failure for %10 probability of exceeding in 50-years earthquake intensity measure were calculated as %97, %23, %3 and %0 for slight, moderate, large, and collapse, respectively. The results show that simply supported steel truss bridges supports were more vulnerable to slight damage but safer for moderate, large and collapse damage than MSSS steel roadway bridges.

The bridge components were also considered in terms of yielding and collapse. Top wind brace elements were calculated as more vulnerable elements of the truss system and median values were 0.43 g and 0.71 g for yielding and collapse, respectively. Median values for yielding was bigger than MSSS steel roadway bridge slight damage and for a collapse similar to MSSS steel roadway bridge collapse damage. System fragility for yielding of the bridge components was derived. Top wind brace element strongly affected system fragility so the upper and lower bound were close to each other. Probabilities of failure for %10 probability of exceeding in 50-years earthquake intensity measure was obtained as %44 for yielding and as similar to MSSS steel roadway bridge moderate damage.

Acknowledgments

This research presented in this paper was supported by TCDD and TUBİTAK 114M332 project. Any opinions expressed in this paper are those of authors and do not reflect the opinions of the supporting agencies.

References

Baker, J.W. (2015), "Efficient analytical fragility function fitting using dynamic structural analysis", *Earthq. Spectra*, **31**(1), 579-599. https://doi.org/10.1193/021113EQS025M.

Banerjee, S. and Shinozuka, M. (2007), "Nonlinear static procedure for seismic vulnerability assessment of bridges", *Comput. Aid. Civil Infrastr. Eng.*, **22**(4), 293-305. https://doi.org/10.1111/j.1467-8667.2007.00486.x.

Bignell, J.L., LaFave, J.M., Wilkey Joseph P. and Hawkins, N. M. (2004), "Seismic evaluation of vulnerable highway bridges with wall piers on emergency routes in Southern Illinois", *13 the World Conference on Earthquake Engineering*, Van-Couver, BC, Canada, August.

Bruneau, M., Wilson, J.C. and Tremblay, R. (1996), "Performance of steel bridges during the 1995 Hyogo-ken Nanbu (Kobe, Japan) earthquake", *Can. J. Civil Eng.*, **23**, 678-713. https://doi.org/10.1139/l2012-045.

Byers, W.G. (2004), "Railroad lifeline damage in earthquakes", *13 the World Conference on Earthquake Engineering*, Vancouver, BC, Canada, August

EN1990-prANNEX A2 : Application for Bridges (2001), EN 1990 -Eurocode: Basis of Structural Design Annex2: Application for Bridges Design.

Kawashima, K. (2012), "Damage of bridges due to the 2011 great east Japan earthquake", *J. JPN Assoc. Earthq. Eng.*, **12**(4), 319-338. https://doi.org/10.5610/jaee.12.4_319.

Kumar, R. and Gardoni, P. (2014), "Effect of seismic degradation on the fragility of reinforced concrete bridges", *Eng. Struct.*, **79**, 267-275. https://doi.org/10.1016/j.engstruct.2014.08.019.

Larsson, T. and Lagerqvist, O. (2009), "Material properties of old steel bridges", *Nordic Steel Construction Conference 2009*, http://www.nordicsteel2009.se/pdf/888.pdf (last access: January 2018).

Lindfeldt, A. (2015), "Railway capacity analysis", KTH Royal Institute of Technology School of Architecture and the Built Environment Department of Trasport Science.

Liu, Y., Paolacci, F. and Lu, D.G. (2017) "Seismic fragility of a typical bridge using extrapolated experimental damage limit states" *Earthq. Struct.*, **13**(6), 599-611. https://doi.org/10.12989/eas.2017.13.6.599.

Mackie, K. and Stojadinović, B. (2001), "Probabilistic seismic demand model for California highway bridges", *J. Bridge Eng.*, **6**, 468-481. https://doi.org/10.1061/(ASCE)1084-0702(2001)6:6(468).

Mander, J., Kim, D., Chen, S. and Premus, G. (1996), "Response of steel bridge bearings to the reversed cyclic loading", Technical Report NCEER 96-0014, Buffalo, NY.

Mander, J.B. (1999), "Fragility curve development for assessing the seismic vulnerability of highway bridges", Available at: http://mceer-nt4.mceer.buffalo.edu/publications/resaccom/99-SP01/Ch10mand.pdf.

Mohseni, M. (2012), "Dynamic vulnerability assessment of highway and railway bridges", Ph.D. Teises, University of Nebraska-Lincoln.

Mosleh, A., Razzaghi, M.S., Jara, J. and Varum, H. (2016), "Development of fragility curves for RC bridges subjected to reverse and strike-slip seismic sources", *Earthq. Struct.*, **11**(3), 517-538. http://dx.doi.org/10.12989/eas.2016.11.3.517.

Nielson, B.G. (2005), "Analytical fragility curves for highway bridges in moderate seismic zones", available at: http://smartech.gatech.edu/handle/1853/7542.

Nielson, B.G. and DesRoches, R. (2007), "Seismic fragility methodology for highway bridges using a component level approach", *Earthq. Eng. Struct. Dyn.*, **36**(6), 823-839. https://doi.org/10.1002/eqe.655.

Padgett, J.E. and DesRoches, R. (2008), "Methodology for the development of analytical fragility curves for retrofitted bridges", *Earthq. Eng. Struct. Dyn.*, **37**(8), 1157-1174. https://doi.org/10.1002/eqe.801.

Pan, Y., Agrawal, A.K. and Ghosn, M. (2007), "Seismic fragility of continuous steel highway bridges in New York state", *J. Bridge Eng.*, **12**(6), 689-699. https://doi.org/10.1061/(ASCE)1084-0702(2007)12:6(689).

Razzaghi, M.S., Safarkhanlou, M., Mosleh, A. and Hosseini, P. (2018), "Fragility assessment of RC bridges using numerical analysis and artificial neural networks", *Earthq. Struct.*, **15**(4), 431-441. https://doi.org/10.12989/eas.2018.15.4.431.

Sfahani, M.G. and Guan, H. (2018), “An extended cloud analysis method for seismic fragility assessment of highway bridges”, *Earthq. Struct.*, **15**(6), 605-616. https://doi.org/10.12989/eas.2018.15.6.605.

Shah, P.M., Stewart, M. and Fok, H. (2009), “Reliability assessment of a typical steel truss bridge”, *7th Austroads Bridge Conference*, Auckland, New Zealand, May.

Shinozuka, M., Feng, M.Q., Kim, H. and Kim, S. (2000a), “Nonlinear static procedure for fragility curve development”, *J. Eng. Mech.*, **126**, 1287-1295. https://doi.org/10.1061/(ASCE)0733-9399(2000)126:12(1287).

Shinozuka, M., Freg, M.Q., Lee, J. and Naganuma, T. (2000b), “Statistical analysis of fragility curves”, *J. Eng. Mech.*, **126**, 1224-1231. https://doi.org/10.1061/(ASCE)0733-9399(2000)126:12(1224).

Siqueira, G.H., Sanda, A.S., Paultre, P. and Padgett, J.E. (2014), “Fragility curves for isolated bridges in eastern Canada using experimental results”, *Eng. Struct.*, **74**, 311-324. https://doi.org/10.1016/j.engstruct.2014.04.053.

Sisi, A.A., Erberik, M.A. and Askan, A. (2018), “The effect of structural variability and local site conditions on building fragility functions”, *Earthq. Struct.*, **14**(4), 285-295. https://doi.org/10.12989/eas.2018.14.4.285.

Tsionis, G. and Fardis, M.N. (2014), Fragility Functions of Road and Railway Bridges Chapter 9.

Vamvatsikos, D. and Allin Cornell, C. (2002), “Incremental dynamic analysis”, *Earthq. Eng. Struct. Dyn.*, **31**(3), 491-514. https://doi.org/10.1002/eqe.141.

Yazgan, U. (2015), “Empirical seismic fragility assessment with explicit modeling of spatial ground motion variability”, *Eng. Struct.*, **100**, 479-489. https://doi.org/10.1016/j.engstruct.2015.06.027.

Yılmaz, M.F. and Çağlayan, B.Ö. (2018), “Seismic assessment of a multi-span steel railway bridge in Turkey based on nonlinear time history”, *Nat. Hazard. Earth Syst. Sci.*, **18**(1), 231-240. https://doi.org/10.5194/nhess-18-231-2018.

CC